Copy
RM L57D23c

4

NACA RM L57D23c

C1

RESEARCH MEMORANDUM

FLUTTER EXPERIMENTS WITH VARIOUS CONTROL CONFIGURATIONS

By Robert W. Boswinkle, Jr., and Homer G. Morgan

Langley Aeronautical Laboratory
Langley Field, Va.

NATIONAL ADVISORY COMMITTEE
FOR AERONAUTICS

WASHINGTON

July 10, 1957

NACA RM L57D23c

NATIONAL ADVISORY COMMITTEE FOR AERONAUTICS

RESEARCH MEMORANDUM

FLUTTER EXPERIMENTS WITH VARIOUS CONTROL CONFIGURATIONS

By Robert W. Boswinkle, Jr., and Homer G. Morgan

SUMMARY

The flutter characteristics of various control-surface configurations have been under study at the Langley Aeronautical Laboratory. Presented herein is a compilation of some of the more pertinent results. Most of the models studied were dynamically and elastically scaled from proposed aircraft. The flutter investigations were made in various facilities over both the transonic and supersonic speed ranges. Configurations tested included a wing with tip ailerons, all-movable elevators, vertical tails with trailing-edge rudders, and a T-tail.

INTRODUCTION

A large portion of the flutter problems which plague modern aircraft is associated with control systems. No really reliable analytical method is available for designing controls in the transonic zone. Such a variety of configurations arise that an overall trend study of characteristics is impractical. The alternative is to investigate experimentally the various specific configurations as they arise. Much of the work on controls at the Langley Aeronautical Laboratory has been of this type.

The Langley Laboratory has worked with various organizations on control-surface flutter problems of new aircraft. The work has included transonic and supersonic flutter tests of models. Most of the models used were both dynamically and elastically scaled from the prototype aircraft. Some of the more pertinent results of these investigations will be presented. The controls to be discussed are shown as configurations A to H in figure 1. They include a wing with tip ailerons, two all-movable controls, four vertical tails with trailing-edge rudders, and a T-tail.

SYMBOLS

a	speed of sound, ft/sec
b	root half chord, ft

g structural damping coefficient

M Mach number

q dynamic pressure, lb/sq ft

V free-stream velocity, ft/sec

$$\mu = \frac{\text{Mass of wing}}{\text{Mass of air contained in truncated cone determined by wing}}$$

ω_f flutter frequency, radians/sec

ω_h bending frequency, radians/sec

ω_α torsional frequency, radians/sec

ω_β control-surface rotational frequency, radians/sec

ω_θ pitch frequency of all-movable control, radians/sec

ω_1 first coupled frequency, radians/sec

DISCUSSION

Configuration A - Wing With Tip Ailerons

Configuration A was a wing of arrowhead plan form, shown in figure 1, with trailing-edge flaps and all-moving tip ailerons. The leading edge of the wing was swept back 55° and the trailing edge was swept rearward 10°. The aileron was about 20 percent of the exposed wing area and its hinge line was swept back about 4.5°. The hinge line was located at 56 percent of the aileron root chord (where the aileron root chord is the chord which contains the innermost parting line). The airfoil was 3 percent thick. The wing was cantilever mounted at the root. The trailing-edge flaps had a fixed rotational stiffness. Flutter points were obtained for different values of simulated aileron actuator stiffness.

The results are shown in figure 2, plotted as the stiffness-altitude parameter against Mach number. Increases in altitude correspond to increases in the value of the stiffness-altitude parameter. In this type figure, constant altitude occurs as a horizontal line, and constant-dynamic-pressure curves are straight lines through the origin. In figure 2, the frequency in the stiffness-altitude parameter is the torsion frequency of the wing. The actuator stiffness is the actual value divided by the original value.

Data for the original value of actuator stiffness are shown on the left side of figure 2. The no-flutter points correspond to about sea-level conditions. The mode of flutter which occurred at a Mach number of about 0.9 was predominantly bending and torsion of the wing, whereas the flutter mode at supersonic Mach numbers was predominantly aileron rotation.

These flutter points were considered to be too close to the airplane flight regime and an improvement in the conditions was sought by increasing the actuator stiffness to three times the original stiffness. This increased actuator stiffness was still a feasible value. The data obtained with the stiffer actuator are shown by the squares on the right side of figure 2. The no-flutter points at supersonic speeds so obtained were at lower altitudes than the flutter points previously obtained with the lower actuator stiffness. No-flutter points were also obtained at supersonic speeds with an infinite actuator stiffness. Infinite actuator stiffness was simulated by gluing the aileron to the wing so no relative motion could take place. It is interesting to note, however, that, even with infinite actuator stiffness, bending-torsion-type flutter was still obtained near a Mach number of 0.9 and occurred at about the same altitude as for the lowest value of actuator stiffness.

Increasing the actuator stiffness was one way to increase the aileron rotation frequency; another way was to reduce the moment of inertia of the aileron. Since there was considerable windup of the ailerons, a large reduction in effective moment of inertia was possible by cutting off the tips of the ailerons. Accordingly, the tips were cut off along the dashed lines shown in figure 1. Removal of these tips gave beneficial results at supersonic speeds but again left the subsonic flutter region essentially unaffected.

Increasing the actuator stiffness or cutting off the aileron tips reduced the altitude at which the aileron-rotation-type flutter occurred at supersonic speeds. These changes had no effect on the bending-torsion-type flutter obtained at subsonic speeds.

Configuration B - All-Movable Stabilizer

Configuration B, as shown in figure 1, was an all-movable stabilizer. The model had an aspect ratio of 3.3, a taper ratio of 0.42, 35° sweepback of the quarter-chord line, airfoil sections tapering from 6 percent thick at the root to 4 percent at the tip, a rounded tip, and a pitch axis at 78.9 percent of the center-line chord. Tests were made at a constant value of stabilizer twist stiffness and ratio of bending frequency to torsion frequency. The pitching frequency of the stabilizer on its spindle was the main test variable.

These test results are shown in figure 3 where the stiffness-altitude parameter is shown as a function of Mach number for various values of the ratio of bending frequency to pitch frequency. The frequency in the stiffness-altitude parameter is the torsion frequency of the stabilizer. The lower curve is for a frequency ratio of 0.50. As the Mach number is increased, the flutter boundary shifts to higher altitudes. This Mach number effect becomes more pronounced as the frequency ratio is increased toward 1.0, as shown by the slopes of the curves for frequency ratios of 0.62, 0.77, and 0.94.

The effect of frequency ratio at a Mach number of 0.8 is shown in figure 4. The flutter-speed coefficient $V/b\omega_\alpha$ is plotted as a function of frequency ratio for a given value of mass-density ratio. It should be noted that on this plot the flutter side of the boundary is above the curve. The experimental data are shown as a solid curve, cross-plotted from the previous figure. The other two curves are calculated results using two-dimensional incompressible aerodynamic coefficients and three uncoupled modes. The calculations were made at a fixed value of the ratio of bending frequency to torsion frequency, $\omega_h/\omega_\alpha = 0.305$. The lower dashed-line curves assume zero structural damping coefficient and the upper dashed-line curves use a structural damping coefficient in each of the three modes equal to the measured values. This calculation again shows the importance of damping on flutter speeds at frequency ratios near 1. The trend at frequency ratios below 1 appears to be predicted and the calculations are on the conservative side of the boundary. The calculations predict a favorable jump in flutter speed as the frequency ratio is increased above 1 although experimental data were not obtained at large enough frequency ratios for verification. For frequency ratios above 1, these calculations indicate that the flutter speed increases almost directly with the torsion frequency. Changes in ratio of bending frequency to pitch frequency would have practically no effect on the flutter speed. However, at frequency ratios between about 0.3 and 0.8, increases in torsion frequency may not result in proportionate increases in flutter speed. The flutter speed in this region varies in a much more complicated manner. For example, notice that an increase in torsion frequency ω_α while holding the ratio of bending frequency to torsion frequency constant would require increases in ω_h, the bending frequency. This, in turn, would increase the ratio of bending frequency to pitch frequency and lower the flutter-speed coefficient. A more complete discussion of this behavior is given in reference 1.

Configuration C - All-Movable Stabilizer

Configuration C, shown in figure 1, is a statically balanced all-movable stabilizer. The control was spindle mounted with the rotation

axis at 46 percent of the root chord. Its semispan aspect ratio was 1.56, leading-edge sweepback was 20°, the trailing edge was swept forward 24°, and the thickness ratio was 5 percent. Torsion frequency of the surface was very high, so that the predominant control-surface modes were pitch about the spindle axis and bending. Studies were made at various values of the ratio of bending frequency to pitch frequency. The results are shown in figure 5, with stiffness-altitude parameter plotted as a function of Mach number. The frequency in the stiffness-altitude parameter is the rotation frequency of the stabilizer. The upper curve is the flutter boundary established for an uncoupled bending-pitch frequency ratio of 1.02. When the frequency ratio was increased to 1.41 or decreased to 0.92, favorable shifts in the flutter boundary were obtained. For the higher frequency ratios the flutter mode involved both bending and torsion, whereas for the lowest frequency ratio the flutter mode involved primarily bending. These tests demonstrate that a change in frequency ratio which moves the frequency ratio away from 1 is beneficial and requires less stiffness to avoid flutter.

Mass balancing is a common method for increasing the flutter speed of controls. Such a method was studied for this case. The results are shown in figure 6. The plain-wing data for a frequency ratio of 1.02 are repeated from the previous figure. Also shown is the flutter boundary obtained when a heavy leading edge was added to the same configuration on the outboard 50 percent of the control, as shown by the sketch in figure 6. The added weight was about 7 percent of the plain-wing weight. The frequency ratio of the modified model dropped to 0.95. Adding the weight is seen to be beneficial so that less stiffness is required to prevent flutter. However, the increase in flutter speed may be due to the change in frequency ratio as well as the center-of-gravity shift.

Calculations have been made for comparison with the experimental data obtained with the plain wing at frequency ratios of 1.02 and 1.41. The calculated and experimental results are compared in figure 7. Experimental flutter points are shaded symbols and experimental no-flutter points are open symbols. The calculated results are shown as the curves. These calculations used the first two measured coupled modes of the system. Zero structural damping was assumed and the aerodynamic forces were obtained from piston theory (ref. 2) including the effect of airfoil thickness.

The calculated flutter boundary for a frequency ratio of 1.02 is seen to be in excellent agreement with the experimental data over the Mach number range investigated - 1.5 to 2.8. The agreement is not so good for a frequency ratio of 1.41. For this case, the calculated curve passes through experimental no-flutter points at Mach numbers of 1.6 and 2.0 and so predict more stiffness than necessary. Not enough stiffness is predicted at a Mach number of 2.2. These two examples give some

indication of the reliability of low supersonic flutter-speed calculations using piston theory. For one case, agreement between experiment and calculations is good and in the other case, not so good.

Configurations D and E - Vertical Tails With Trailing-Edge Rudders

Configurations D and E, shown in figure 1, were swept vertical tails with unbalanced trailing-edge rudders. Studies were made in two different facilities to obtain the flutter boundary for each configuration at both transonic and supersonic speeds. The models were cantilever mounted and had fairings to keep them out of the tunnel boundary layer. The models were flat plates that were tapered in thickness along the span. Both models had 60° sweptback leading edges. Vertical tail D had a panel aspect ratio of 0.72 and a taper ratio of 0.43. Its rudder hinge line was swept back 43° and its rudder was 24 percent of the exposed surface area. Vertical tail E had a panel aspect ratio of 0.77 and a taper ratio of 0.48, based on a plan form without a rounded tip. Its rudder hinge line had 50° of sweepback and its rudder was about 36 percent of the exposed surface.

The results for configuration D are presented in figure 8, where the stiffness-altitude parameter is plotted as a function of Mach number. The frequency appearing in the stiffness-altitude parameter is the rotation frequency of the rudder. This model was cantilever mounted along its entire root chord. These controls had a ratio of first bending frequency to rudder-rotational frequency of about 0.4. Also shown in figure 8 is the flutter frequency referred to the control rotation frequency. At a Mach number of about 1.2, an abrupt increase in stiffness is required to prevent flutter. At the same Mach number the flutter frequency also changes abruptly. At lower Mach numbers, the flutter frequency is less than the rudder-rotation frequency, whereas at higher Mach numbers the flutter frequency is greater than the rudder-rotation frequency. This change in flutter frequency is associated with a change in the flutter mode. Previously, flutter mode changes in wings without controls have been observed to produce more stable configurations in the transonic region. In the present case, however, the change is toward a less stable system.

Figure 9 shows the results for configuration E wherein the plan form was cantilevered from a stub. In this case, the ratio of first-bending frequency to rudder-rotation frequency is about 0.3. Again, the figure shows both the stiffness-altitude parameter and ratio of flutter frequency to rudder-rotation frequency as functions of Mach number. The flutter frequency again suggests a change in the flutter mode past a Mach number of 1 but the change is gradual as Mach number increases and not abrupt as

for configuration D. Also, no destablizing jump or discontinuity in the stiffness-altitude parameter occurs as Mach number increases. If a flutter-mode change does occur, the shift is gradual and produces no detrimental effects.

For vertical tail D, a destablizing jump was found in the flutter boundary at low supersonic speeds, whereas none was obtained for vertical tail E. A very different type of flutter boundary was obtained for somewhat similar vertical tails with rudders. However, for both controls, if the surface were designed with just enough stiffness to avoid flutter at transonic Mach numbers, a new flutter region would be encountered at the same altitude at a Mach number of about 2.5. This again shows the existence of two critical flutter regions - transonic and supersonic. A complete description and discussion of the tests on these two vertical tails will be found in reference 3.

Configurations F and G - Vertical Tails With Trailing-Edge Rudders

Configurations F and G, shown in figure 1, were swept vertical tails with statically balanced trailing-edge rudders. Static balancing was accomplished with overhanging-balance weights located at the top of the rudders. Vertical tail F had an aspect ratio of 1.33, taper ratio of 0.44, and its rudder was about 24 percent of the exposed surface area. Vertical tail G had an aspect ratio of 1.58, a taper ratio of 0.40, and a rudder which was about 20 percent of the exposed surface area. Both configurations had 45° sweep at the quarter-chord line, 29° sweep on their rudder hinge lines and tapered in thickness from about 6 percent at the root to about 4 percent at the tip. The models were cantilever mounted at the root.

The results for vertical tail F are presented in figure 10. The frequency appearing in the stiffness-altitude parameter is the torsion frequency of the fin. Fin properties remained essentially unchanged during the test, while the actuator and rudder twist stiffnesses were varied. The actuator and twist stiffnesses shown in the figure have been divided by the values of the stiffnesses for the original configuration. The flutter points obtained with the original vertical tail are indicated by the circles. This flutter boundary fell within the airplane flight regime. In an attempt to study the nature of this flutter, a new system was tried wherein the rudder twist stiffness was increased to 1.3 times the original value while actuator stiffness was reduced to 0.8 of its value. The squares show where flutter was obtained with the changed stiffnesses. They show that the change was quite detrimental to the flutter boundary; that is, with a stiffer rudder and a weaker actuator the flutter boundary shifted to higher altitudes. The coupled frequency

spectrum of the two models remained about the same: $\omega_\beta/\omega_\alpha = 0.33$ and $\omega_h/\omega_\alpha = 0.22$.

Some tests were made with viscous dampers on the original rudder in an attempt to eliminate the flutter from the flight envelope of the airplane. The dampers were mounted at about midspan on the rudder. Flutter was still obtained when the damping produced by the dampers was 60 percent of critical. The flutter was eliminated when the damping was 120 percent of critical. The damping values quoted here are based on an inelastic rudder and back-up structure. Since these assumptions yield high values of critical damping, the damping actually obtained was probably somewhat less than the stated value.

The circles for the original vertical tail are repeated as circles again in figure 11 where dynamic pressure is shown as a function of Mach number. For this plot the flutter side of the boundary is above the curve. Also shown in this figure are three no-flutter points and a flutter point obtained with vertical tail G which had a longer and stiffer fin than vertical tail F. As indicated in the figure, the rudder actuator and twist stiffness for vertical tail G were also somewhat greater than for vertical tail F, although ω_h/ω_α and $\omega_\beta/\omega_\alpha$ were about the same. These results indicate that the flutter boundary for vertical tail G would be at substantially higher dynamic pressures than for vertical tail F. However, the one flutter point for vertical tail G was still considered to be too close to the airplane flight regime. An adequate flutter boundary appeared to be obtained when viscous dampers were used. The dampers produced about 15 percent of critical damping.

An additional test was made without dampers but with the fin tip cut off along the dashed line indicated in figure 1. With the fin tip cut off, vertical tail G had about the same plan form as vertical tail F but the frequency ratios were reduced to $\omega_\beta/\omega_\alpha = 0.25$ and $\omega_h/\omega_\alpha = 0.18$. The one flutter point obtained with the fin tip cut off, shown in figure 11, reveals a large increase in dynamic pressure required to flutter this tail compared with vertical tail F. This increase in dynamic pressure required to flutter the clipped configuration G over that required for configuration F can be attributed to increases in the stiffness of the fin, actuator, and rudder. The rudder twist stiffness was 2.8 times that of the original configuration and the actuator stiffness was 1.5 times that of the original configuration.

Studies of vertical tails F and G in the transonic speed range have shown that their flutter boundaries are sensitive to changes in the rudder twist stiffness and rudder actuator stiffness. Flutter could be eliminated by using viscous dampers, but the amount of damping required varied greatly between the two configurations.

Configuration H - T-tail

Configuration H, shown in figure 1, is a T-tail which did not have any movable control surfaces. The torsion and side flexibilities of the fuselage were simulated in the tail mounts. The fin had an aspect ratio of 1.0, a taper ratio of 0.56, and 45° sweepback of the quarter-chord line. The stabilizer had an aspect ratio of 1.8, a taper ratio of 0.43, and 40° sweepback of the quarter-chord line. The ratio of cantilevered fin bending to fin torsion frequencies was about 0.55.

The results of the flutter investigation are shown in figure 12. Stiffness-altitude parameter is plotted as a function of Mach number and the frequency appearing in the parameter is the torsion frequency of the fin. The original stabilizer had 15° of positive dihedral and the flutter points obtained with this configuration are indicated by the circles. Models with zero stabilizer dihedral were also investigated and the flutter points obtained with this configuration are indicated by the squares. The results indicate that less fin stiffness is required for zero stabilizer dihedral and so stabilizer dihedral is indicated to be detrimental.

The detrimental effect of stabilizer dihedral can be explained qualitatively by considering the stabilizer as a yawing wing. When the fin twists, the stabilizer yaws. As a result of dihedral this yaw motion produces a rolling moment on the stabilizer so that fin twist results in fin bending.

Simple Models of All-Movable Controls

In addition to the previously discussed scaled models, some simple models of all-movable controls have been investigated at low supersonic speeds. As figure 13 shows, they had arrowhead plan forms - a 45° delta and one with a 45° sweptback leading edge and a 15° sweptforward trailing edge. The models were flat plates with beveled edges and were supported by a shaft mounted in a bearing. The flexibility was primarily in the shaft so that the control surface experienced only rigid-body torsion, flapping, and translation. The ratios of first coupled frequency to second coupled frequency varied from about 0.3 to about 0.7.

The results are presented as the stiffness-altitude parameter plotted against rotation-axis position in percent of root chord. The frequency in the stiffness-altitude parameter is the first coupled frequency of the system. The trend shown at a Mach number of 1.2 for both surfaces produces a more stable configuration as the rotation axis is moved forward. The two flutter points obtained at a Mach number of 1.6 indicate that, for rearward rotation axes, more stiffness is required to prevent flutter as

the Mach number increases. However, the stiffness required at a Mach number of 1.6 rapidly decreases as the rotation axis is moved forward so that, at the axis location shown in the figure, the controls were stable at a zero value of the stiffness-altitude parameter. This means the controls were flutter free when unrestrained in rotation and when free to float. Thus, these results show that movement of the axis location forward was beneficial on these plan forms at low supersonic Mach numbers.

CONCLUDING REMARKS

A compilation of flutter experiments with various control configurations at transonic and supersonic speeds has been presented. Some trends on specific configurations are indicated and improvements in flutter characteristics for various cases are shown. It would be risky to draw general conclusions from these results, but the discussion should be of value.

Langley Aeronautical Laboratory,
National Advisory Committee for Aeronautics,
Langley Field, Va., March 7, 1957.

REFERENCES

1. Land, Norman S., and Abbott, Frank T., Jr.: Transonic Flutter Investigation of an All-Movable Horizontal Tail for a Fighter Airplane. NACA RM L56G06, 1957.

2. Ashley, Holt, and Zartarian, Garabed: Piston Theory - A New Aerodynamic Tool for the Aeroelastician. Jour. Aero. Sci., vol. 23, no. 12, Dec. 1956, pp. 1109-1118.

3. Hanson, Perry W., and Rainey, A. Gerald: Experimental Investigation of the Transonic and Supersonic Flutter Characteristics of the Upper and Lower Vertical Tails of an Air-to-Ground Missile. NACA RM L57D17, 1957.

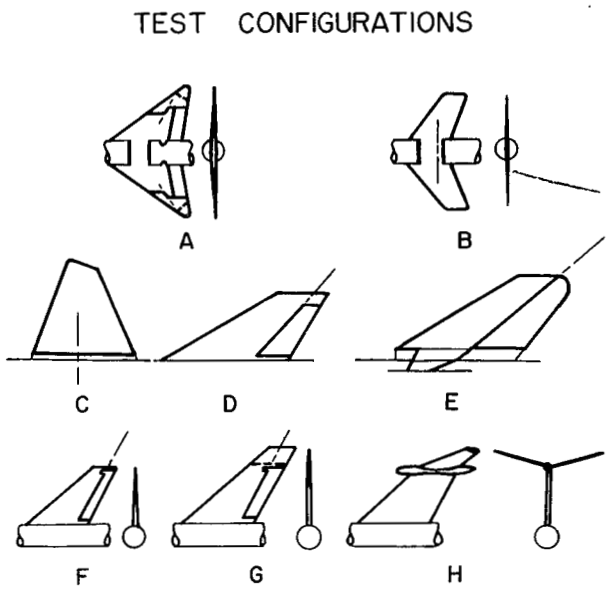

Figure 1

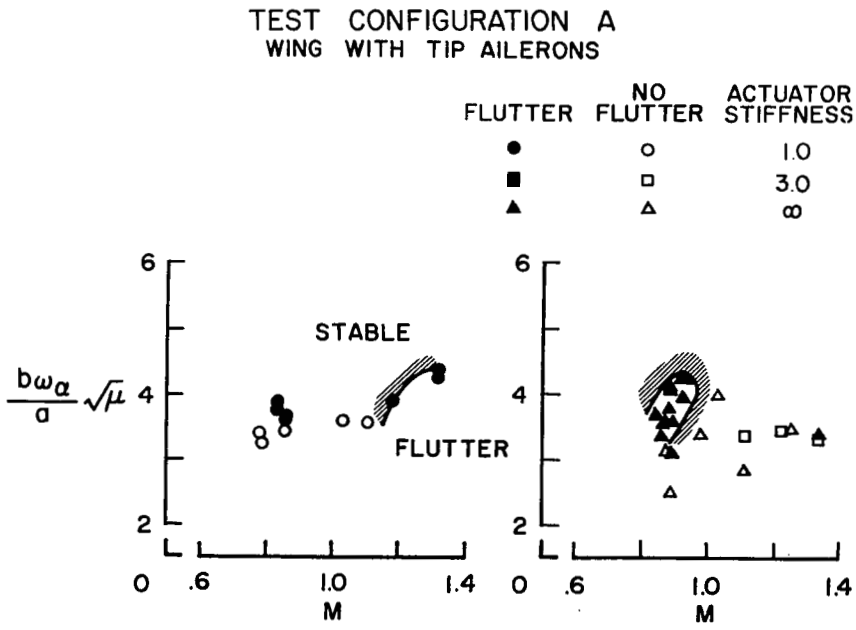

Figure 2

TEST CONFIGURATION B
ALL-MOVABLE STABILIZER

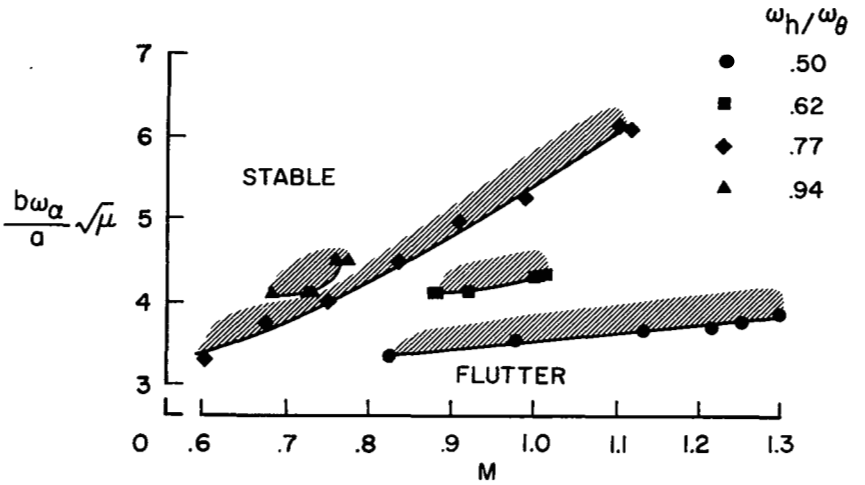

Figure 3

TEST CONFIGURATION B
ALL-MOVABLE STABILIZER

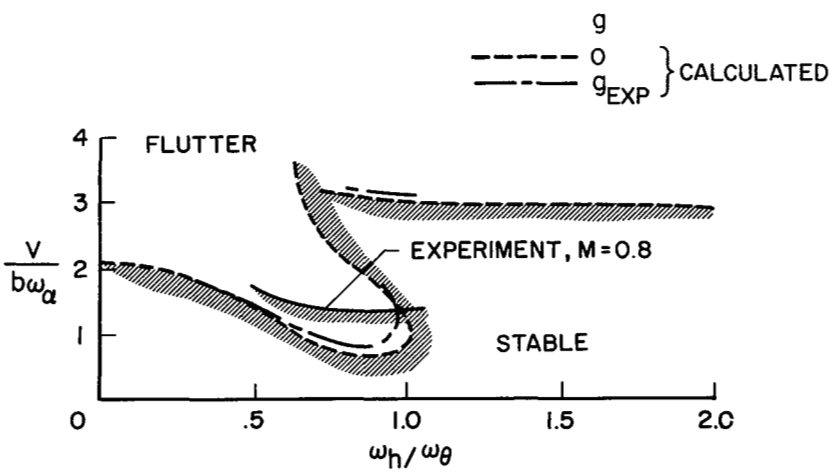

Figure 4

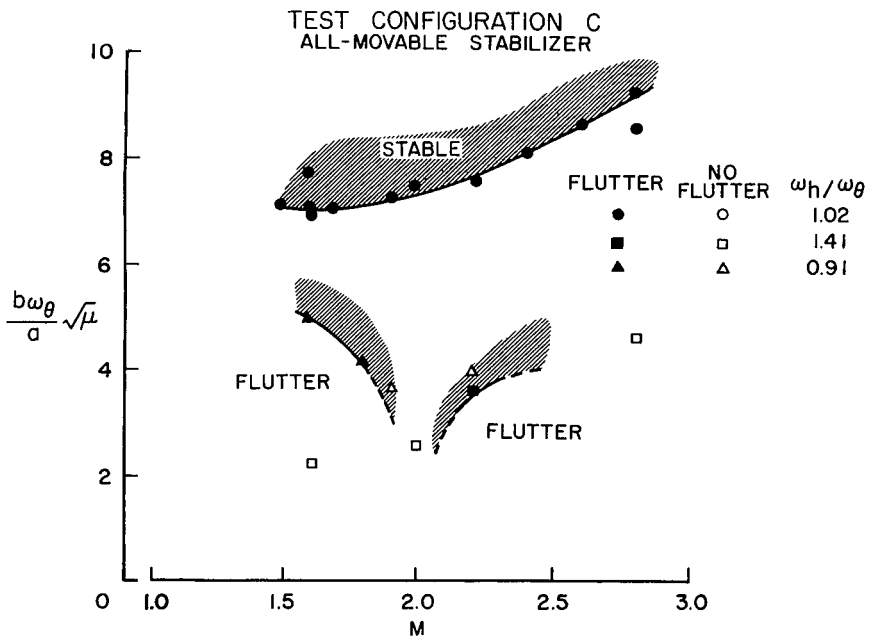

Figure 5

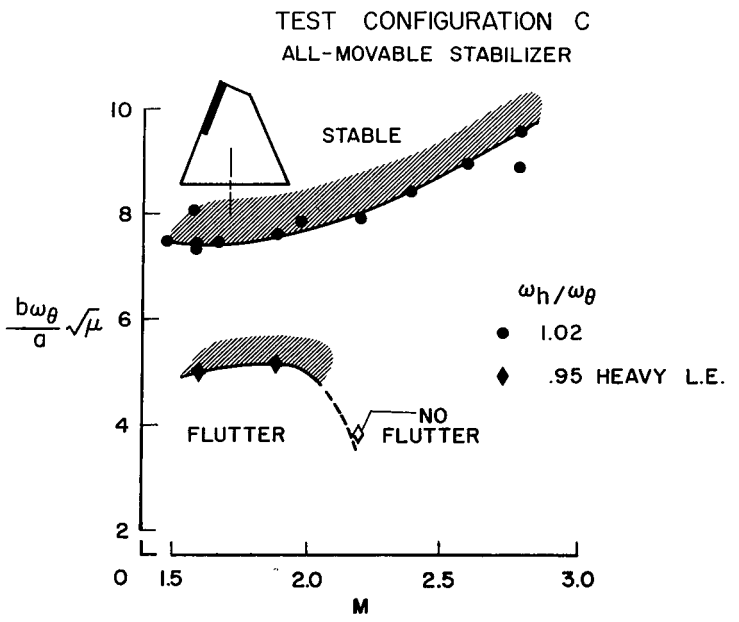

Figure 6

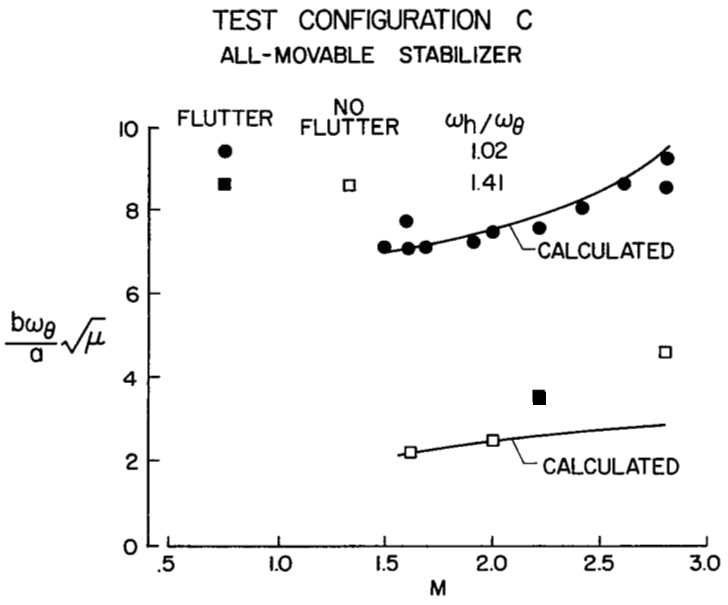

Figure 7

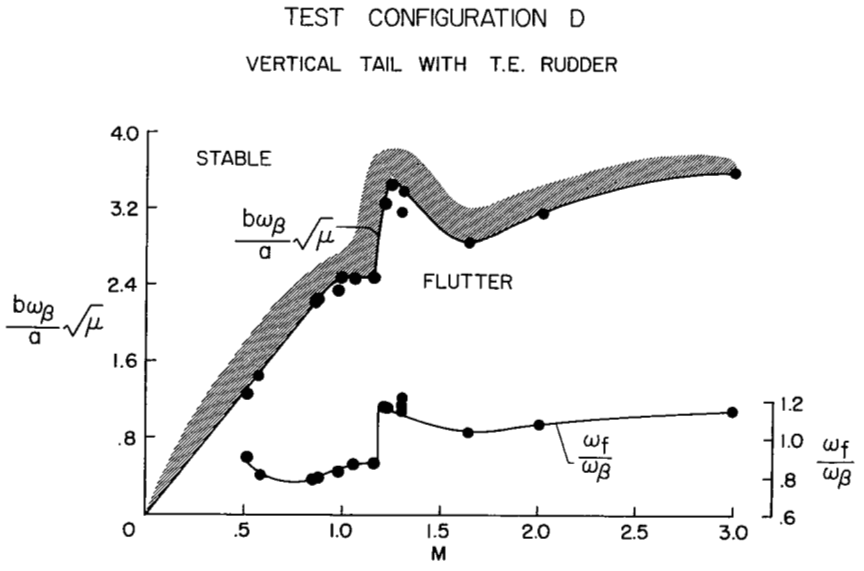

Figure 8

TEST CONFIGURATION E
VERTICAL TAIL WITH T.E. RUDDER

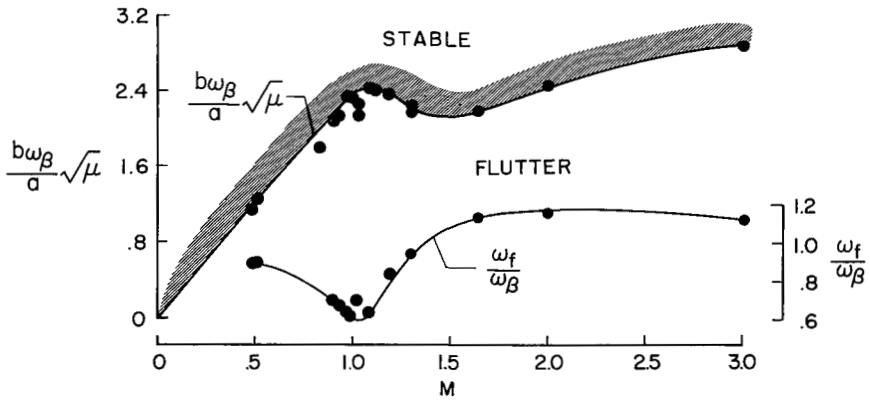

Figure 9

TEST CONFIGURATION F
VERTICAL TAIL WITH T.E. RUDDER

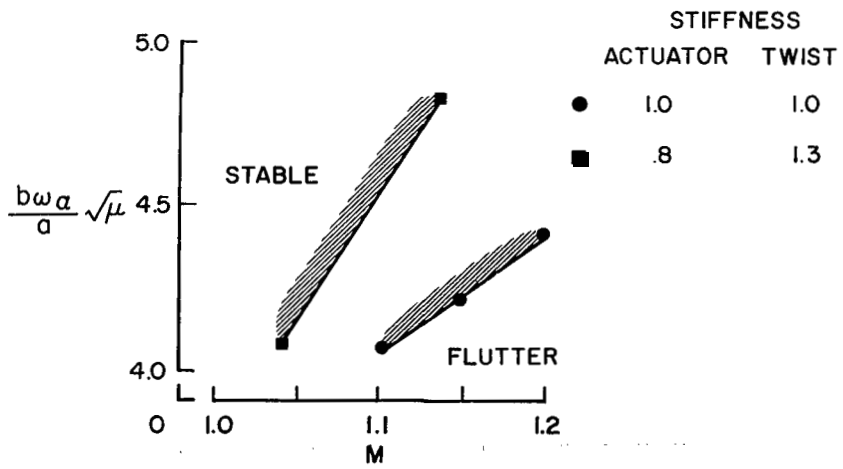

Figure 10

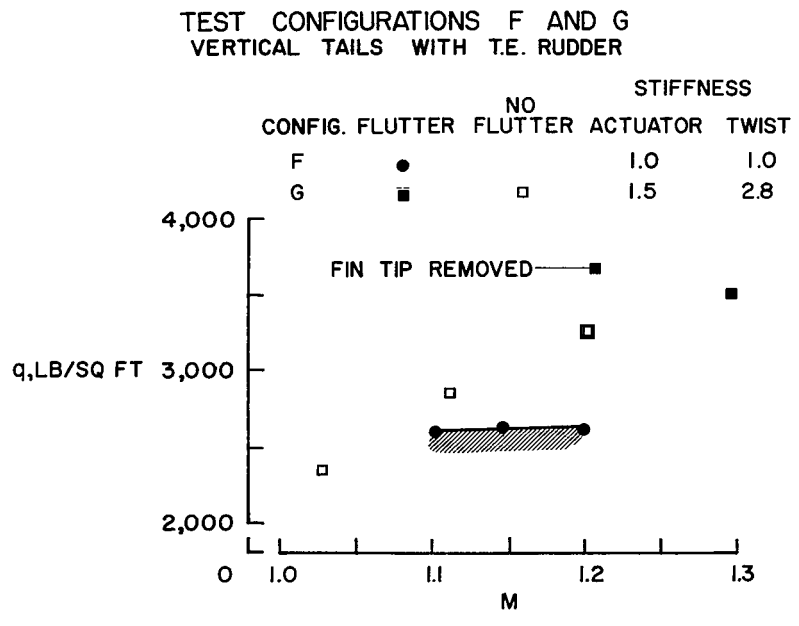

Figure 11

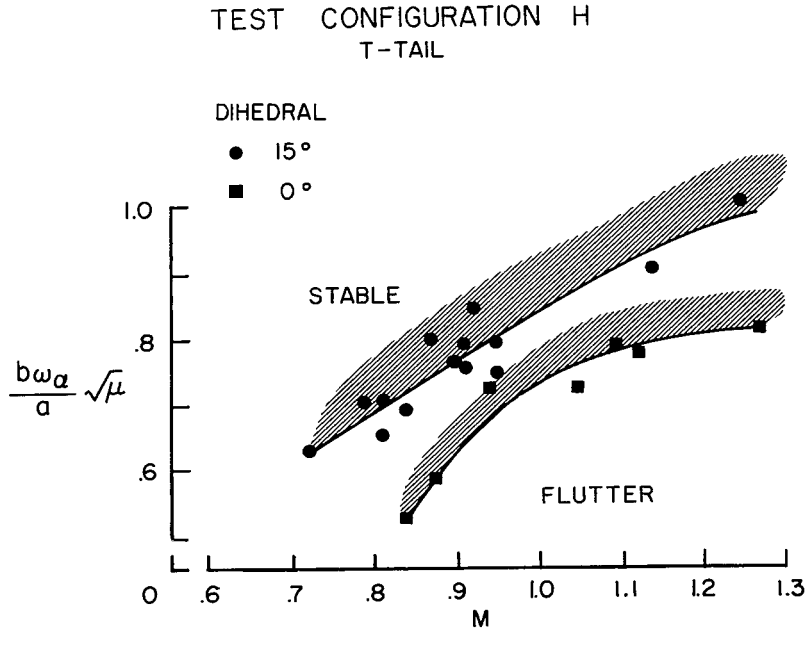

Figure 12

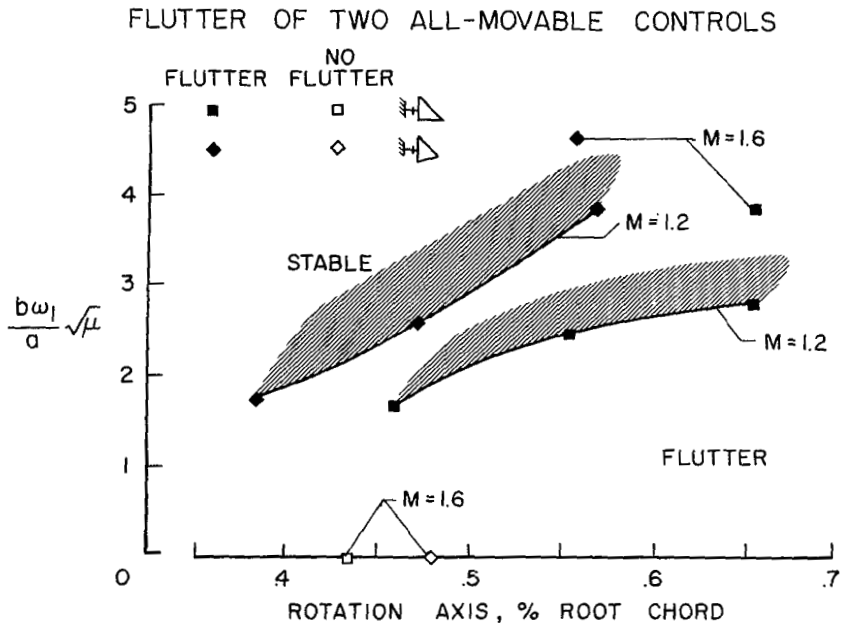
FLUTTER OF TWO ALL-MOVABLE CONTROLS
NO FLUTTER
FLUTTER
M = 1.6
M = 1.2
STABLE
M = 1.2
FLUTTER
M = 1.6
$\frac{b\omega_1}{a}\sqrt{\mu}$
5
4
3
2
1
0
.4
.5
.6
.7
ROTATION AXIS, % ROOT CHORD

Figure 13